UC Berkeley
UC Berkeley Previously Published Works

Title

Lhx6 Directly Regulates Arx and CXCR7 to Determine Cortical Interneuron Fate and Laminar Position

Permalink

https://escholarship.org/uc/item/60c1t5jc

Journal

Neuron, 82(2)

ISSN

0896-6273

Authors

Vogt, Daniel
Hunt, Robert F
Mandal, Shyamali
et al.

Publication Date

2014-04-01

DOI

10.1016/j.neuron.2014.02.030

Peer reviewed

Lhx6 Directly Regulates *Arx* and *CXCR7* to Determine Cortical Interneuron Fate and Laminar Position

Daniel Vogt[1,*], **Robert F. Hunt**[2], **Shyamali Mandal**[1,3], **Magnus Sandberg**[1], **Shanni N. Silberberg**[1], **Takashi Nagasawa**[4], **Zhengang Yang**[5], **Scott C. Baraban**[2], and **John L.R. Rubenstein**[1,*]

[1]Department of Psychiatry, Neuroscience Program and the Nina Ireland Laboratory of Developmental Neurobiology, University of California San Francisco, San Francisco, CA 94158, USA

[2]Epilepsy Research Laboratory, Department of Neurological Surgery, University of California, San Francisco, San Francisco, CA 94143, USA

[3]Department of Cancer Biology and Pharmacology University of Illinois, Peoria, IL 61656, USA

[4]Department of Immunology and Hematology, Institute for Frontier Medical Sciences, Kyoto University, 53 Kawahara-cho, Shogoin, Sakyo-ku, Kyoto 606-8507, Japan

[5]Institutes of Brain Science, Fudan University, Shanghai 200032, China

SUMMARY

Cortical GABAergic interneurons have essential roles for information processing and their dysfunction is implicated in neuropsychiatric disorders. Transcriptional codes are elucidating mechanisms of interneuron specification in the MGE (a subcortical progenitor zone), which regulate their migration, integration, and function within cortical circuitry. Lhx6, a LIM-homeodomain transcription factor, is essential for specification of MGE-derived somatostatin and parvalbumin interneurons. Here, we demonstrate that some Lhx6$^{-/-}$ MGE cells acquire a CGE-like fate. Using an in vivo MGE complementation/transplantation assay, we show that Lhx6-regulated genes Arx and CXCR7 rescue divergent aspects of Lhx6$^{-/-}$ cell-fate and laminar mutant phenotypes and provide insight into a neonatal role for CXCR7 in MGE-derived interneuron lamination. Finally, Lhx6 directly binds in vivo to an Arx enhancer and to an intronic CXCR7 enhancer that remains active in mature interneurons. These data define the molecular identity of Lhx6 mutants and introduce technologies to test mechanisms in GABAergic interneuron differentiation.

INTRODUCTION

Disruptions in the balance of cortical excitation and inhibition are implicated in epilepsy, cognitive disorders, social dysfunction, and autism spectrum disorder (Chao et al., 2010; Cobos et al., 2005; Han et al., 2012; Rubenstein and Merzenich, 2003; Yizhar et al., 2011). In the forebrain most inhibition is generated by GABAergic interneurons, whereas glutamatergic projection neurons and thalamic afferents generate most cortical excitation. Multiple subgroups of GABAergic interneurons modulate distinct components of cortical circuits, in part through their physiological and molecular properties as well as their connectivity (Huang et al., 2007). In rodents, cortical interneurons arise from the subcortical medial and caudal ganglionic eminences (MGE and CGE, respectively) (Anderson et al., 1997; Wonders and Anderson, 2006), and the preoptic area (POA) (Gelman et al., 2011). The MGE gives rise to somatostatin (SST)$^+$ and parvalbumin (PV)$^+$ interneurons, while the CGE gives rise to vasoactive intestinal peptide (VIP)$^+$, serotonin receptor (5Ht3a)$^+$, Reelin$^+$; SST$^-$, and Sp8$^+$ interneurons (Cai et al., 2013; Kanatani et al., 2008; Lee et al., 2010; Ma et al., 2012; Rudy et al., 2011).

MGE identity is specified by the Nkx2-1 homeodomain transcription factor (TF), in part by inducing the expression of Lhx6 and Lhx8 LIM-homeodomain TFs (Sussel et al., 1999). Lhx6 and Lhx8 are coexpressed in the MGE subventricular zone (SVZ), where they have partially redundant functions (Flandin et al., 2011). Tangentially migrating and mature interneurons maintain Lhx6, but not Lhx8, expression (Grigoriou et al., 1998; Sussel et al., 1999). *Lhx6* mutants exhibit many phenotypes, including drastic reductions in SST$^+$ and PV$^+$ cortical interneurons, slowed tangential migration, and abnormal neocortical laminar position of interneurons. After tangential migration to the developing neocortex, MGE- and CGE-derived interneurons preferentially sort into deep and superficial layers, respectively, during neonatal ages (Miyoshi and Fishell, 2011). However, MGE-derived interneurons from *Lhx6* mutants fail to occupy middle neocortical layers and exhibit a preference for superficial and very deep layers (Liodis et al., 2007; Zhao et al., 2008). While Lhx6 promotes the expression of several genes that control cell fate and migration, including *Arx, Sox6, CXCR7* (Flandin et al., 2011; Zhao et al., 2008), and *Satb1* (Close et al., 2012; Denaxa et al., 2012), only the role of *Satb1* in the *Lhx6* phenotype has been evaluated.

We investigated the molecular and physiological phenotype of *Lhx6* mutant MGE cells and cortical interneurons. A subset of *Lhx6* mutant MGE cells exhibit molecular, functional, and laminar properties of CGE-like interneurons, particularly those in layer I that resemble the neurogliaform subgroup. To further characterize *Lhx6* mutant cells, we developed a complementation/transplantation assay. Lentiviral-delivered genes are directed by cell-type-specific enhancers to MGE cells, allowing for the evaluation of in vivo phenotypes of transduced cells following transplantation into the neocortex. Restoration of *Arx* expression rescued the PV and SST phenotypes, while expression of CXCR7 partially rescued the lamination phenotype. We provide evidence that CXCR7 promotes the ability of transplanted interneurons to integrate into neocortical layer V. Finally, LHX6 directly binds enhancers near *Arx* and *CXCR7*, and this *CXCR7* enhancer drives expression in MGE-derived interneurons into postnatal stages.

RESULTS

Lhx6 Represses CGE-like Identity in MGE Cells

One hypothesis to explain the drastic loss of SST^+ and PV^+ interneurons and laminar deficits in *Lhx6* mutants (Liodis et al., 2007; Zhao et al., 2008) is that Lhx6 controls the regional fate of MGE cells. Thus, we tested whether $Lhx6^{PLAP/PLAP}$ mutant MGE cells expressed transcripts normally enriched in LGE- and/or CGE-derived cells: Sp8, COUPTFII (NR2F2), and 5HT3aR (Cai et al., 2013; Kanatani et al., 2008; Ma et al., 2012; Rudy et al., 2011), or the dorsal MGE marker cMaf (McKinsey et al., 2013). At E15.5, Sp8 was ectopically expressed in the MGE subventricular zone (SVZ) of *Lhx6* mutants (Figure 1A), but we did not observe changes in COUPTFII, 5HT3aR, and cMaf (Figures S1A–S1C available online). These results suggest a partial shift in molecular identity of mutant cells toward LGE/CGE fate. Similarly, in postnatal day (P) 14 or 17, brains of *Lhx6* mutants, 5HT3aR, COUPTFII, and c-Maf RNA expression were unaltered (Figures S1D–S1I and S1D′–S1I′), but numbers of $Sp8^+$ cells were increased in the neocortex at P17 (Figures 1B, 1F, 1K, and 1L: total p = 0.02, superficial II/III p = 0.02, deep p = 0.02).

Next, we assessed markers of CGE-derived (VIP) or CGE- and MGE-derived (CR and reelin) interneurons in P17 *Lhx6* mutants. The number and distribution of VIP^+ interneurons (Figures 1C, 1G, 1K, and 1M) was unchanged and CR^+ interneurons decreased ~3-fold (Figures 1D, 1H, 1K, and 1N: total p = 0.0004, superficial II/III p = 0.0005, deep p = 0.003). Reelin marks cortical interneurons in superficial neocortical layers (mostly CGE-derived) and deep layers (mostly MGE-derived) (Alcántara et al., 1998; Miyoshi et al., 2010). Total $reelin^+$ cells were reduced in *Lhx6* mutants (Figures 1E, 1I, and 1K: p = 0.009), especially in deep layers (Figure 1O: p = 0.0002). However, $reelin^+$ cells were significantly increased 1.3-fold in layer I (Figure 1O: superficial I p = 0.02). Together, these data show that *Lhx6* mutants exhibit an early and persistent increase in the number of interneurons expressing SP8, a CGE-derived interneuron marker, without any change in the number of VIP^+ interneurons. The concurrent decrease of reelin in deep layers, coupled with an increase in superficial layers ($reelin^{sup}$), is consistent with a loss of "MGE-type" interneurons and an increase in "CGE-type" interneurons.

Transplanted *Lhx6*^{PLAP/PLAP} MGE-Derived Interneurons Exhibit Cell Autonomous Deficits in Cell Fate and Lamination

To test if known $Lhx6^{PLAP/PLAP}$ cortical phenotypes are cell autonomous and to further examine changes in molecular and laminar phenotypes, we used an MGE transplantation assay (Alvarez-Dolado et al., 2006; Cobos et al., 2005). E13.5 *CAG-dsRed* (Vintersten et al., 2004) MGE cells were transplanted into P1 wild-type (WT) neocortex and allowed to mature (Figure S2A). At 25 days posttransplant (DPT), similar numbers of control and $Lhx6^{PLAP/PLAP}$ transplanted $dsRed^+$ cells were detected in the neocortex (data not shown), and ~60% of control and mutant transplanted cells expressed the neuronal marker NeuN by this time point, (Figures S2B–2D). Very few *Lhx6* mutant transplanted cells expressed SST (Figure S3D: p = 0.001) and PV (Figure S2D: p = 0.002).

Next, we quantified the proportion of dsRed^{+} cells residing in layer I, compared to all layers. The majority of control cells were distributed throughout layers II–VI with few at the lower border of layer I, whereas nearly half of the *Lhx6* mutant cells were found in layer I (Figure S2E: p = 5.2 × 10^{-7}). Thus, transplanted *Lhx6$^{PLAP/PLAP}$* cells recapitulate the cortical phenotypes found in the mutant mouse line, demonstrating that these defects are cell autonomous.

To further test the hypothesis of an MGE to CGE-like cell fate switch, we performed in vivo fate mapping studies using *Nkx2-1-Cre* (Xu et al., 2008) and the Cre-indicator line AI14, in which recombination activates expression of tdTomato (Madisen et al., 2010). *Nkx2-1-Cre; Lhx6$^{PLAP/+}$* mice were crossed to *Lhx6$^{PLAP/+}$;AI14* mice, and we assessed for Sp8 and reelin in P13 tdTomato^{+} neocortical cells. In controls, many tdTomato^{+} cells were found in deep layers and did not express Sp8, however, ~13% of the *Lhx6$^{PLAP/PLAP}$* tdTomato^{+} cells expressed Sp8 (p = 0.002), ~22% of which were in layer I (Figures 2A–2F and 2N).

Next, we assessed the laminar position of reelin^{+} cells that were in the *Nkx2-1*-lineage. Approximately 70% of the reelin^{+} cells in deep layers (IV–VI) were tdTomato[+] (Figure 2M), indicating that the majority of these cells are MGE/POA-derived. *Lhx6$^{PLAP/PLAP}$* brains had a decrease in the total number of tdTomato[+]/reelin^{+} cells (Figures 2K, 2L, and 2O, p = 0.0008). Furthermore, while controls had very few (<2%) of tdTomato[+]/reelin^{+} cells in layer I, ~45% of *Lhx6$^{PLAP/PLAP}$* mutant cells were in layer I (Figure 2P, p = 0.002). Thus, we propose that a subset of *Lhx6$^{PLAP/PLAP}$* MGE-derived interneurons acquire molecular and laminar properties resembling CGE-derived interneurons (Sp8^{+} and reelin[sup]).

Lhx6P$^{LAP/PLAP}$ MGE-Derived Interneurons Exhibit Late-Spiking Electrophysiological Properties

Lhx6 mutants are small and die before P18, prior to when the electrophysiology of interneurons can be reliably assessed. To circumvent this lethality and potential non-cell-autonomous effects, we generated a lentivirus, *DlxI12b-GFP*, to express genes specifically in forebrain GABAergic neurons (Arguello et al., 2013). Previous analyses showed that the *DlxI12b* enhancer is active in progenitors that generate the majority of forebrain GABAergic neurons (Ghanem et al., 2003; Potter et al., 2009). We transduced MGE cells with *DlxI12b-GFP* lentivirus, and then transplanted them into a WT host and allowed them to mature in vivo (Figure 3A). To test the efficiency of this approach, we transduced E13.5 *CAG-dsRed* MGE cells with *DlxI12b-GFP* lentivirus (Figure S3A), and then transplanted them into P1 cortices. The *DlxI12b* enhancer is active throughout development and into adult stages. At 10 DPT, we found that ~50% of dsRed^{+} cells were effectively transduced and expressed GFP (Figures S3C–S3E).

Next, we transplanted control and *Lhx6* mutant MGE cells transduced with *DlxI12b-GFP* lentivirus into P1 WT neocortex, and performed patch-clamp recordings of DlxI12b-GFP^{+} cells in acute cortical slices at 35 DPT, (example cells, Figure 3B). Current injections into control and *Lhx6$^{PLAP/PLAP}$* cells revealed four types of firing patterns: fast spiking, regular spiking, burst spiking, and late spiking (Figure 3C). All recorded neurons displayed electrophysiological properties consistent with functionally mature inhibitory neurons (Table S1), and both the passive membrane properties and active firing of each subgroup

were comparable to previously described values (Miyoshi et al., 2010;Tricoire et al., 2011). Importantly, ~50% of the mutant cells (5/10) in layer I exhibited late-spiking properties (7/16, layers 1– 3), whereas no control grafted cells had this property (0/18; all layers) (Figures 3D and 3D′). The layer I $Lhx6^{PLAP/PLAP}$ cells expressed GABA (data not shown). We also observed a few fast spiking neurons derived from $Lhx6$ mutant cell grafts (3/25), suggesting that a few grafted mutant cells retain this property of MGE-derived interneurons.

Voltage-clamp recordings (−70 mV) detected spontaneous excitatory postsynaptic currents (EPSCs) in all control and mutant grafted interneurons (Figures 3C, 3E, and 3E′), consistent with their functional integration into the host neocortex. EPSCs were more frequent in fast spiking neurons compared to other subgroups (Table S1). In contrast, late-spiking neurons received low-frequency EPSCs that had relatively small amplitudes and fast rise-times (Table S1), features previously reported for late spiking neurogliaform cells (Chu et al., 2003; Armstrong et al., 2011) and layer I neurons (Zhou and Hablitz, 1997). However, for each interneuron subgroup identified on the basis of electrophysiological properties (e.g., fast spiking) we found no gross differences in the EPSC characteristics between mutants and controls (Table S1). Thus, $Lhx6$ mutant MGE cells differentiated into physiologically mature GABAergic cortical interneurons that were functionally similar to controls, except that a large fraction of mutant interneurons exhibited late-spiking properties, a feature of neurogliaform interneurons (Miyoshi et al., 2010). Together, these electrophysiological, molecular (reelin and Sp8 expression), and laminar (neocortical layer I) properties indicate that many of the layer I $Lhx6$ mutant MGE cells resemble neurogliaform interneurons.

Rescue of $Lhx6^{PLAP/PLAP}$ MGE Interneuron Fate via Transduction of Lhx6-Regulated Genes

$Lhx6$ is necessary for the expression of Arx and $Sox6$ TFs and the $CXCR7$ cytokine receptor (Batista-Brito et al., 2009; Flandin et al., 2011; Zhao et al., 2008). $Lhx8$ MGE function is partially redundant for $Lhx6$ (Flandin et al., 2011). To test if these factors were sufficient to complement specific $Lhx6$ phenotypes, we developed an approach to transduce MGE cells before transplantation with a modified $DlxI12b-GFP$ lentivirus that also encoded these genes (Figure 4A, schema). The genes were inserted downstream of a T2a element in the viral vector (Figure S3A), and the expression of each protein was confirmed (Figure S3B).

E13.5 MGE cells (control or $Lhx6^{PLAP/PLAP}$) were transduced with $DlxI12b-GFP$, transplanted, and assessed at 35 DPT. GFP⁺ control transplants expressed SST (~50%) and PV (~23%) at expected frequencies (Figures 4B, 4H, 4N, and 4O). GFP-transduced $Lhx6^{PLAP/PLAP}$ transplants had a drastic reduction in SST⁺ (~2%) and PV⁺ (~3%) interneurons (Figures 4B′, 4H′, 4N′, and 4O′), recapitulating the $Lhx6^{PLAP/PLAP}$ phenotypes.

$Lhx6$ transduction into $Lhx6$ mutant MGE cells rescued SST and PV expression to approximately WT levels (Figures 4C, 4I′, 4N′, and 4O′: SST p = 4.01×10^{-10}, PV p = 0.0002). Thus, despite a delayed onset of expression ($Lhx6$ expression is initiated in WT mice at ~E10.5), rescued cells still differentiate with properties of MGE-derived interneurons. Moreover, like $Lhx6$, $Lhx8$ transduction of $Lhx6$ mutant MGE cells rescued PV (Figures 4J′ and 4O′: p = 0.0002), and mostly rescued SST (Figures 4D′ and 4N″: p = 1.88×10^{-7}). $Lhx8$ promotes development of telencephalic choline acetyltransferase (ChAT)

neurons (Zhao et al., 2003; Fragkouli et al., 2009). However, expression of *Lhx8* did not induce ectopic ChAT expression in transplanted MGE cells (Figures S4A–S4G). On the other hand, *Lhx8* transduction restored SOX6 expression in the *Lhx6* mutant cells (Figures S4H–S4O), providing further evidence for its redundancy with *Lhx6*.

Arx and *Sox6* expression in *Lhx6* mutant MGE appears normal, but is not maintained in tangentially migrating MGE cells (Zhao et al., 2008). *Sox6* transduction rescued neither SST (Figures 4F′ and 4N′) nor PV expression (Figures 4L′ and 4O′). In contrast, *Arx* transduction of *Lhx6* mutant MGE cells restored ~25% of the SST cells (Figures 4E′ and 4N′: p = 0.01) and ~80% of the PV cells (Figures 4K′ and 4O′: p = 0.002). Denaxa et al. (2012) found that *Satb1* is downstream of *Lhx6* and promotes SST expression. We also detected loss of Satb1 expression in *Lhx6* mutants (Figures S5A–S5F) but *Arx* transduction did not rescue Satb1 expression in *Lhx6* mutants (Figures S5G–S5L).

CXCR7 expression in the *Lhx6* mutants is greatly reduced in the MGE and tangentially migrating MGE cells (Zhao et al., 2008). Transduction of CXCR7 into *Lhx6* mutant MGE cells rescued neither SST (Figures 4G′ and 4N′) nor PV (Figures 4M′ and 4O′) expression, but did partially rescue the lamination phenotype (see next section).

Transducing *Lhx6*, *Lhx8*, or *Arx* into control MGE cells did not significantly change the numbers of interneuron subgroups (Figures 4C–4E, 4I–4K, 4N, and 4O). However, transduction of *Sox6* and *CXCR7* altered the numbers of SST$^+$ and PV$^+$ interneurons. *Sox6* increased SST$^+$ cells (Figure 4N: p = 0.04) and concurrently promoted a trend for decreased PV$^+$ cells (Figure 4O). This effect was more pronounced in *Lhx6$^{+/+}$* cells (SST p = 0.0002, PV p = 0.01) than *Lhx6$^{PLAP/+}$* cells (SST p = 0.008, PV p = n.s.) (data not shown). Of note, control MGE cells transduced with *CXCR7* generated normal numbers of SST$^+$ cells (Figures 4G and 4N), but ~50% reduction of PV$^+$ cells (Figures 4M and 4O: p = 0.005).

Together, these data show that while *Lhx6*, *Lhx8*, and *Arx* were sufficient to rescue *Lhx6$^{PLAP/PLAP}$* SST and PV phenotypes, *Sox6* did not rescue these deficits. However, gain-of-function assays suggest *CXCR7* and *Sox6* dosage may regulate the SST/PV ratio, the latter is consistent with *Sox6* loss-of-function data (Azim et al., 2009; Batista-Brito et al., 2009).

Lamination Defects of *Lhx6$^{PLAP/PLAP}$* Interneurons Are Rescued by *Lhx6, Lhx8*, and *CXCR7*

Lhx6 mutant interneurons have abnormal laminar positions in the postnatal neocortex, mostly occupying superficial and very deep layers (Liodis et al., 2007; Zhao et al., 2008). We found that this laminar phenotype is cell autonomous, as many transplanted E13.5 *Lhx6* mutant interneurons occupy superficial layers (Figure S2). We next asked if *Lhx6*, or its downstream factors, could rescue the laminar phenotype (layer I localization) of *Lhx6* mutant cells, by assessing the proportion of transplanted cells in layer I at 35 DPT transduced with *GFP-*, *Lhx6-*, or *Lhx6*-regulated factors.

Control MGE cells, transduced with *GFP-, Lhx6-*, or *Lhx6*-regulated factors, rarely (~10%) were found in neocortical layer I (Figure 5A), with the majority at the I/II border. By

contrast, half of the *GFP*-transduced, *Lhx6* mutant MGE cells occupied layer I (Figure 5B). Transduction of *Lhx6* or *Lhx8* decreased mutant cells found in layer I to control levels (Figure 5B: Lhx6, p = 0.002; Lhx8 p = 0.0005). Transduction of *Arx* or *Sox6* did not rescue the laminar distribution (Figure 5B). However, transduction of *CXCR7* induced an ~2-fold reduction of cells in layer I (Figure 5B: p = 0.01), suggesting that reduced levels of *CXCR7* contributes to the *Lhx6^{PLAP/PLAP}* laminar phenotype.

Lhx6 Transduction Partially Rescues *Lhx6^{PLAP/PLAP}* CGE-like Characteristics

Transduction of *Arx* and *CXCR7* rescued divergent aspects of the *Lhx6* mutant phenotypes, perhaps via suppression of CGE-like molecular phenotypes. Thus, we first assessed reelin expression in transduced MGE transplants at 35 DPT (Figures 5C–5J). GFP transduction recapitulated the previous phenotypes (Figures 1 and 2), with *Lhx6* mutants exhibiting ~30% reduction in reelin$^+$ cells (Figures 5C, 5G, 5K, and 5K′) and ~60% in neocortical layer I (Figure 5L′). Transduction of *Lhx6* into *Lhx6^{PLAP/PLAP}* MGE cells increased the total number of reelin$^+$ cells (Figures 5H and 5K': p = 0.009) and reduced reelin$^+$ cells in layer I ~20-fold (Figure 5L′: p = 0.0001). *CXCR7* transduction induced an ~2-fold reduction of reelin$^+$ cells in layer I (Figure 5L′: p = 0.005). Transduced control cells did not show changes in reelin$^+$ cell numbers (Figure 5K), although reelin$^+$ cells in layer I were reduced by *Lhx6* and *Arx* transduction (Figure 5L: Lhx6 p = 0.002; Arx p = 0.02). Despite changes in reelin, ectopic Sp8 was still observed in transplanted *Lhx6* mutant MGE cells transduced with either *Lhx6, Arx, CXCR7 or GFP* (Figure S6 and data not shown), suggesting that a full reversal of CGE properties did not occur. Despite the inability of *Lhx6* to reverse the ectopic expression of Sp8, *Lhx6* transduction increased the total number of reelin$^+$ interneurons, and decreased reelin$^+$ interneurons in layer I (Figures 5K′ and 5L′). Moreover, while *Arx* and *CXCR7* were sufficient to restore MGE molecular and laminar properties in the *Lhx6* mutants, neither were able to rescue the reelin phenotype as completely as *Lhx6*, suggesting that additional *Lhx6*-regulated factor(s) contribute to this process.

Transplanted MGE Cells Lacking CXCR7 or CXCR4 Exhibit Deficits in Integration into Neocortical Layer V

The ability of *CXCR7* to rescue the laminar position of *Lhx6^{PLAP/PLAP}* interneurons (Figure 5B) prompted us to ask if *CXCR7* influenced transplanted MGE cell integration into deep neocortical layers. The chemokine CXCL12 is the principal ligand for CXCR7; its prenatal expression in the cortical meninges and intermediate zone attracts immature cortical interneurons expressing CXCR4 and CXCR7, promoting their tangential migration along superficial and deep pathways, and preventing their premature entry into the cortical plate (Sánchez-Alcañiz et al., 2011; Stumm et al., 2003; Wang et al., 2011). Later, CXCL12 mRNA is present in deep cortical layers in the neonatal brain (Schönemeier et al., 2008; Stumm et al., 2003), and GFP expression from the CXCL12 locus (Ara et al., 2003) reveals postnatal expression in neocortical layer V pyramidal neurons (Figures S7A–S7C). We hypothesized that postnatal expression of CXCL12 may influence the laminar distribution of transplanted MGE cells by attracting some transplanted MGE cells into neocortical layer V. Toward assessing this, we investigated the laminar position of transplanted MGE cells lacking either *CXCR7* or *CXCR4* at two time points: 7 DPT, when cells are still migrating; 30 DPT, when cells are nearly mature.

First, E13.5 *CAG-dsRed*+ (controls), or *CAG-dsRed*+; *CXCR7*−/− (Sierro et al., 2007) MGE cells were transplanted into P1 *CXCL12-GFP* neocortices and laminar position was assessed at 7 DPT (Figure 6A, schema). Because *CXCR7* mutants have little to no CXCR4 protein (Sánchez-Alcañiz et al., 2011), the mutant interneurons should lose their ability to respond to CXCL12. At 7 DPT, the *CXCR7*−/− interneurons accumulated in superficial layers and were reduced in layer V (Figures 6B–6D, $p < 0.001$).

To test if *CXCR7*−/− interneuron laminar deficits persist in the adult cortex, and to explore whether CXCR4 and CXCR7 have different functions, we transplanted E13.5 *Lhx6-GFP*+ MGE cells from control, *CXCR4*−/− or *CXCR7*−/− embryos (Figure 6E). Analysis at 30 DPT revealed that *CXCR4*−/− and *CXCR7*−/− MGE interneurons accumulated in superficial layers and were reduced in layer V (Figures 6F–6I: *CXCR4*−/− and *CXCR7*−/− compared to controls $p < 0.05$). Together, the 7 and 30 DPT data suggest that CXCR4/7-signaling in the neonatal cortex regulates the targeting of some interneurons to layer V.

Because *CXCR7* transduction into WT MGE cells decreased PV+ numbers (Figure 4O), we tested whether loss of *CXCR7* influenced the PV/SST ratio using the MGE transplantation assay. *CXCR7*−/− transplants exhibited a 50% reduction in PV+ cells compared to controls (Figures 6M, 6O, and 6Q: $p = 0.006$). However, *CXCR4*−/− transplants did not exhibit a significant decrease in PV (Figures 6N and 6Q). There were no gross changes in SST levels among groups (Figures 6J–6L and 6P). Thus, in addition to promoting MGE-derived interneuron migration, imbalances in CXCR7 levels, but not CXCR4, may regulate PV interneuron differentiation or maturation.

Lhx6 Directly Binds and Activates *Arx* and *CXCR7* Enhancers

We next asked if *Lhx6* could directly regulate *Arx* and *CXCR7* by screening potential enhancers near their genomic loci (Figure 7A). Enhancers near *Arx* have been identified that are active during telencephalon development (Colasante et al., 2008). An *Arx* enhancer region within the *PolA1* locus drives expression in developing basal ganglia, while regions closer to *Arx* drive expression in embryonic neocortex. We screened the basal ganglia *Arx* enhancer and regions near the *CXCR7* locus using MatInspector to predict sites containing putative Lim-homeodomain binding sites. The *Arx* enhancer contained five sites, (A1–A5), (Figure 7A, top), and several sites were found near *CXCR7*, (C1–C10), including seven in the intron (Figure 7A, bottom).

To test if these sites (Figure 7A, black bars) were bound by Lhx6 in vivo, we generated an antibody against Lhx6 and performed chromatin immunoprecipitation from E13.5 MGEs. *Arx* site A3 showed enrichment over input (Figure 7B: $p = 0.03$), as did sites A2, A4, and A5, whereas site A1 did not show Lhx6 binding (Figure 7B and data not shown). Site C8 in the *CXCR7* intron was also bound by Lhx6 (Figure 7B: $p = 0.007$).

We then tested if Lhx6 and its cofactor Ldb1 could modulate expression from the candidate *CXCR7* intronic enhancer (Figure 7A, red bar). Driving Lhx6/Ldb1 expression in P19 cells led to ~4-fold increase in activity of a luciferase reporter plasmid containing the *CXCR7* intron (PGL4.23-*CXCR7-int*), compared to a control (PGL4.23) plasmid lacking the *CXCR7* intron (Figure 7C: $p = 0.01$).

Finally, we tested the activity of the *CXCR7* intron enhancer in slice culture and in vivo. We inserted the *CXCR7* intron upstream of *GFP*, and in a separate vector we inserted the GABAergic enhancer, *DlxI56i* (Zerucha et al., 2000), upstream of mCherry. We then coelectroporated them into E13.5 tissue slices containing LGE, MGE, and CGE (Figure S8A). While mCherry was detected in the LGE, MGE, and CGE, GFP expression was largely restrict to the MGE (Figures S8B, S8B″, S8D, and S8D″). Moreover, many mCherry^{+} cells migrating out of the MGE expressed GFP, suggesting that the *CXCR7* intron is active in MGE-derived GABAergic interneurons. To test this idea, we examined whether the *CXCR7* intron could drive expression in MGE-derived SST[+] and PV[+] interneurons. E13.5 *AI14*^{+} MGE cells were transduced with a *CXCR7* intron-*GFP*-T2a-*Cre* lentivirus (Figure 7D), transplanted into a P1 WT host and assessed at 35 DPT. At 35 DPT, ~60% of the GFP^{+} cells expressed SST and ~20% expressed PV (Figure 7D). Fate mapped tdTomato^{+} cells marked similar proportions of SST[+] and PV^{+} cells. Furthermore, by dividing the number of GFP^{+} cells by the number of tdTomato^{+} cells, we determined that ~50% of the transduced cells maintained enhancer activity by 35 DPT.

Overall, these data show that Lhx6 directly bound to enhancer elements near *Arx* and *CXCR7*, where it may promote expression of these genes. Furthermore, the newly discovered *CXCR7* intronic enhancer was highly expressed in the MGE, and in mature SST[+] and PV[+] interneurons.

DISCUSSION

Lhx6 mutants have defects in MGE-derived cortical interneuron development, including loss of PV[+] and SST[+] interneurons and a preference to occupy both superficial and very deep neocortical layers (Liodis et al., 2007; Zhao et al., 2008). Previous molecular analyses identified downregulated genes in *Lhx6* mutants that may contribute to these phenotypes, including *Arx, CXCR7, Satb1*, and *Sox6* (Close et al., 2012; Denaxa et al., 2012; Flandin et al., 2011; Zhao et al., 2008). Here, we report aspects of the *Lhx6* molecular phenotype and its downstream genes (Figure 7E, schema). A subset of *Lhx6* mutant MGE-derived cells exhibit molecular and laminar properties of CGE-derived interneurons. Moreover, the reelin^{+} cells in neocortical layer I have properties of neurogliaform interneurons (Miyoshi et al., 2010). Finally, we developed a complementation assay to demonstrate that specific aspects of the *Lhx6* mutant phenotype are rescued by *Arx* and *CXCR7*, revealing functions of these genes in interneuron development.

Lhx6 Represses CGE Interneuron Fate

The rostrodorsal MGE is a major source of PV[+] and SST[+] cortical interneurons (Flandin et al., 2010; Rudy et al., 2011). In *Lhx6* mutants, this progenitor zone maintains many of its normal properties, perhaps because the MGE cells still express *cMaf, Lhx8, Nkx2-1*, and *Sox6* (Flandin et al., 2011; Zhao et al., 2008) (Figure S1). However, in *Lhx6* mutants the rostrodorsal MGE ectopically expressed *Sp8* (Figure 1); *Sp8* ordinarily marks the CGE and LGE, but not the MGE or POA (Ma et al., 2012). These results suggest that *Lhx6* functions not only in the maturation of MGE-derived neurons, but is also required for fate specification of SVZ cells in the rostrodorsal MGE. This is due, in part, to repression of

molecular characteristics of CGE-derived progenitors *(Sp8)* and interneurons (Sp8, reelin[+];SST[−]) (Figures 1 and 2). Moreover, these fate changes are likely cell autonomous, because *Lhx6* mutant MGE cells exhibited similar changes in Sp8 and reelin expression (Figures 5 and S6). A partial fate change may explain why a subset of *Lhx6* mutant cortical interneurons occupy neocortical layer I. While *Lhx6* mutant interneurons in layer I resemble neurogliaform cells, this cell type is not exclusively derived from the CGE, as some come from the MGE (Tricoire et al., 2010). However, we are unaware of MGE-derived interneurons that occupy layer I. Despite these CGE-like properties, *Lhx6* mutant MGE cells did not express other markers of CGE-derived interneuron subgroups, such as 5HT3aR and VIP (Figures 1 and S1) (Lee et al., 2010; Miyoshi et al., 2010), suggesting that these changes in cell fate and laminar position are partial. Overall, these data reveal a role for Lhx6 in mediating MGE interneuron identity and offer insights into the mechanisms underlying *Lhx6* mutant phenotypes.

Arx Functions Downstream of *Lhx6* in Promoting PV and SST Expression

To study the individual functions of genes with reduced expression in *Lhx6* mutants, we developed an MGE complementation assay using lentiviral technology and a cell-type-specific enhancer to rescue phenotypic changes of a specific mutant. We defined rescue as the ability of a transduced factor to restore, or complement, a phenotypic change in mutant cells to control levels. The *DlxI12b* enhancer (Ghanem et al., 2003) can be used in lentiviral vectors to drive gene expression in MGE cells and this enhancer remained active in mature GABAergic interneurons, allowing for assessment at multiple stages of development.

Either *Lhx6* or *Lhx8* transduction can rescue the *Lhx6^{PLAP/PLAP}* phenotypes (Figure 4). Despite transducing cells at E13.5, ~3 days after the MGE would normally begin to express *Lhx6*, the mutant MGE cells maintained sufficient plasticity to be rescued. *Lhx8* transduction in *Lhx6^{PLAP/PLAP}* cortical interneurons enabled them to express PV and SST; thus *Lhx6* and *Lhx8* share some common functions. Interestingly, forced expression of Lhx8 in cortical interneurons restored features associated with Lhx6 expression (Sox6, PV, and SST) rather than inducing cholinergic markers (ChAT) (Figure S4), suggesting that other cofactors may distinguish the cholinergic and GABAergic lineages (e.g., *Isl1* is implicated in the telencephalic cholinergic differentiation) (Elshatory and Gan, 2008; Fragkouli et al., 2009).

Arx transduction into *Lhx6* mutants was sufficient to rescue both SST and PV expression, but it was more efficient at promoting PV[+] interneurons (Figure 4). This difference could be due to the inability of *Arx* to rescue *Satb1* expression in *Lhx6* mutants (Figure S5), as *Satb1* function in MGE interneurons is linked to SST expression (Denaxa et al., 2012; Close et al., 2012).

Arx could promote interneuron differentiation through several molecular pathways. The *Drosophila* Arx (Aristaless) protein binds to Chip, an invertebrate homolog of mammalian Ldb1 (Pueyo and Couso, 2004). Ldb1 is an essential cofactor for Lim-domain homeodomain proteins such as Islet-1, Lhx8, and Lhx6 (Kimura et al., 1999; Y. Zhao and J.L.R.R., unpublished data). Second, in developing muscle, ARX can form a complex with, and enhance the activity of the Mef2C TF (Biressi et al., 2008). Mef2C may have roles in cortical interneuron maturation, as its expression in GABAergic neurons is reduced in

Dlx1/2$^{-/-}$ mutants (Cobos et al., 2007; Long et al., 2009). Thus, Arx may modulate interneuron cell fate through association with Ldb1, Mef2C, or other factors.

Surprisingly, *Sox6* was not sufficient to rescue the *Lhx6* null phenotypes (Figure 4), although *Sox6* is required for development of MGE-derived cortical interneurons (Azim et al., 2009; Batista-Brito et al., 2009). One possibility is that the actions of Sox6 require Lhx6 expression. On the other hand, expression of *Sox6* in control MGE cells increased the ratio of SST/PV-expressing interneurons (Figure 4 and data not shown), suggesting that Sox6 dosage regulates the balance of interneuron subgroups. These data may be of use in furthering methods to program stem cells into specific subgroups of MGE-derived cortical interneurons (Chen et al., 2013; Maroof et al., 2013; Nicholas et al., 2013).

CXCR7 Is a Direct Target of Lhx6 and Modulates Laminar Positioning of Transplanted Interneurons

While *Arx* rescued MGE cell fate, it could not rescue the *Lhx6* mutant lamination phenotype (Liodis et al., 2007; Zhao et al., 2008), in which ~45% of the transplanted mutant interneurons populate neocortical layer I (Figure 5). We propose two mechanisms to explain this abnormal lamination pattern. First, some of these cells exhibit a fate change, acquiring properties of a subset of CGE-derived interneurons that occupy neocortical layer I (Miyoshi et al., 2010). It is also possible that they become POA-like neurogliaform cells (Gelman et al., 2011), although this is less likely based on their expression of Sp8 (Figure 1).

The second mechanism potentially underlying the lamination phenotype is the reduced expression of the CXCR7 and CXCR4 chemokine receptors in *Lhx6* mutant interneurons migrating in the cortex (Zhao et al., 2008). CXCR7 regulates interneuron tangential and radial migration and is required to prevent degradation of CXCR4 (Sánchez-Alcañiz et al., 2011; Wang et al., 2011). We found that transduction of *CXCR7* in *Lhx6* mutants partially rescued the ability of interneurons to exit layer I and integrate into deeper neocortical layers, independent of changes in cell fate (Figures 4 and 5). Transplanted *CXCR4*$^{-/-}$ and *CXCR7*$^{-/-}$ MGE cells were less represented in layer V (Figure 6), suggesting that these receptors participate in radial migration and laminar targeting in the postnatal neocortex. We and others have observed postnatal expression of CXCL12, a CXCR4/7 ligand and interneuron attractant, in layer V pyramidal neurons (Schönemeier et al., 2008; Tiveron et al., 2006; Wang et al., 2011). We hypothesize that postnatal CXCL12 may influence the laminar position of cortical interneurons. However, we are cognizant that the transplantation assay we employed does not recapitulate the normal developmental sequence followed by interneurons; thus in vivo genetic manipulations are needed to test this model. For example, one would selectively eliminate *CXCL12* function in developing layer V, and not in the other locations where it is expressed (marginal and intermediate zones) and then examine interneuron laminar positioning. Ideally, this would be done by deleting CXCL12 at a specific time and cell type (i.e., only in early postnatal layer V pyramidal neurons).

Use of the MGE Complementation Assay to Determine Gene Functions, Coding and Regulatory, in Interneuron Development

We propose that the MGE complementation assay has broad utility to elucidate in vivo functions of candidate alleles. MGE cells are ideally suited for this approach because they can be harvested prenatally, easily transduced, and transplanted in the cortex, where they migrate, differentiate, and functionally integrate (Alvarez-Dolado et al., 2006). This type of complementation and MGE transplantation assay was used to assess the role of Lhx6 in the *Nkx2.1* mutant (Du et al., 2008). Here, we modified this approach by transducing genes using lentiviruses with enhancer elements that drive expression specifically in GABAergic neurons. Importantly, this assay can be used to test the functions of WT genes whose expression is downregulated in a given mutant (as in this article and Du et al., 2008). Alternatively, one can compare the ability of mutant alleles, discovered in human genetic analyses of neuropsychiatric disorders, to rescue phenotypes as compared to WT alleles. Thus, this technique provides a powerful in vivo approach to test a number of molecular mechanisms.

Furthermore, this approach can be used to assay enhancers. Previously, we presented evidence that Lhx6, with Lhx8, regulates a forebrain *Shh* enhancer in MGE neurons (Flandin et al., 2011). Here, we have shown that Lhx6 directly regulates two genes whose functions substantively contribute to the Lhx6 null phenotype: *Arx* and *CXCR7*. Chromatin immunoprecipitation-quantitative PCR (ChIP-qPCR) data identified Lhx6 binding to a previously known *Arx* subpallial enhancer (also regulated by Dlx2) (Colasante et al., 2008), and a *CXCR7* enhancer (Figure 7). This enhancer preferentially drives expression in the MGE, compared to the other basal ganglia primordia (Figure S8). Moreover, by using the MGE-transplantation assay to assess cells transduced with the *CXCR7* enhancer, we found that it drives expression in SST and PV interneurons into adulthood (Figure 7). We propose that this approach to assay enhancer functions will accelerate the identification of regulatory elements that control expression in immature and mature cortical interneurons and should be useful to test the activity of enhancer variants discovered in human genetic analyses of neuropsychiatric disorders.

EXPERIMENTAL PROCEDURES

Animals

Mice were maintained on a CD-1 background. For timed pregnancies, noon on the day of the vaginal plug was counted as embryonic day 0.5. All mice strains have been previously reported: *AI14* Cre-reporter (Madisen et al., 2010), *CXCL-12-GFP* (Ara et al., 2003), *CXCR7*$^{-/-}$ (Sierro et al., 2007), *CXCR4*$^{-/-}$ (Jackson Laboratory 004341), *Lhx6-PLAP* (Choi et al., 2005), *Lhx6 BAC-GFP* (GENSAT), and *Nkx2-1-Cre* (Xu et al., 2008). All animal care and procedures were performed according to the University of California at San Francisco Laboratory Animal Research Center guidelines.

ChIP-qPCR

ChIP was performed on E13.5 basal ganglia using ~4 mg of Lhx6 polyclonal antibody (Genscript), and 20-fold excess of blocking peptide used as a negative control. The

antibody/protein complexes were processed according to the Millipore-Upstate ChIP protocol, and qPCR analyzed as described (Vokes et al., 2007). See the Supplemental Experimental Procedures for detailed methods.

Electrophysiology

Coronal sections were prepared from P35 transplanted mice and assessed as described in Hunt et al. (2013). See the Supplemental Experimental Procedures for detailed methods.

Histology

In situ hybridization on 20 um cryosections was performed as previously described (Jeong et al., 2008). Immunofluorescence was performed on 25 um cryosection as previously described (Zhao et al., 2008). See the Supplemental Experimental Procedures for list of probes, detailed methods, and reagents.

Image Acquisition and Analysis

Fluorescent images were taken using a Coolsnap camera (Photometrics) mounted on a Nikon Eclipse 80i microscope using NIS Elements acquisition software (Nikon). Brightfield images were taken using a DP70 camera (Olympus) mounted to an Olympus SZX7 microscope. Brightness and contrast were adjusted and images merged using ImageJ software.

In Situ Hybridization

Coronal cryostat sections were prepared and processed as described in Jeong et al. (2008). Briefly, E15.5 brains were fixed in 4% paraformaldehyde (PFA) then sunk in 30% sucrose before cutting 20 μm sections. The Sp8 probe has been previously reported (C. Belmonte).

Lentiviral Production

HEK293T cells grown in DMEM H21 with 10% FBS were transfected using Fugene 6 (Promega) with the lentiviral vector and three helper plasmids (pVSV-g, pRSVr, and pMDLg-pRRE). Media was filtered after 4 days in culture and ultracentrifuged at $100,000 \times g$ for 2.5 hr at 4°C and the lentiviral pellet re-suspended in PBS before use. See the Supplemental Experimental Procedures for details on lentiviral vectors.

Luciferase Assays

P19 cells were seeded at density of 100,000 cells/cm^2 in MEM + nucleosides supplemented with 2.5% FBS and 7.5% CS. Cells were transfected at 24 hr with 500 ng total of a DNA mix containing firefly luciferase, transcription factor, and Renilla luciferase vectors. Cells were harvested 48 hr later and assessed for luciferase activity according to Dual luciferase-reproter assay system protocol (Promega).

MGE Transplantation

E13.5 MGE transplantations were done as previously described (Alvarez-Dolado et al., 2006; Cobos et al., 2005). Briefly, MGEs were mechanically dissociated, pelleted, and transplanted into P1 host neocortices or transduced with concentrated lentivirus before

transplantation. For transduction, MGE cells were incubated with lentivirus in media for 30 min at 37°C and then washed with media three times before transplantation. Each host received three to four injections of ~70 nl per site. See the Supplemental Experimental Procedures for detailed methods.

Supplementary Material

Refer to Web version on PubMed Central for supplementary material.

Acknowledgments

References

Alcántara S, Ruiz M, D'Arcangelo G, Ezan F, de Lecea L, Curran T, Sotelo C, Soriano E. Regional and cellular patterns of reelin mRNA expression in the forebrain of the developing and adult mouse. J Neurosci. 1998; 18:7779–7799. [PubMed: 9742148]

Alvarez-Dolado M, Calcagnotto ME, Karkar KM, Southwell DG, Jones-Davis DM, Estrada RC, Rubenstein JLR, Alvarez-Buylla A, Baraban SC. Cortical inhibition modified by embryonic neural precursors grafted into the postnatal brain. J Neurosci. 2006; 26:7380–7389. [PubMed: 16837585]

Anderson SA, Eisenstat DD, Shi L, Rubenstein JLR. Interneuron migration from basal forebrain to neocortex: dependence on Dlx genes. Science. 1997; 278:474–476. [PubMed: 9334308]

Ara T, Tokoyoda K, Sugiyama T, Egawa T, Kawabata K, Nagasawa T. Long-term hematopoietic stem cells require stromal cell-derived factor-1 for colonizing bone marrow during ontogeny. Immunity. 2003; 19:257–267. [PubMed: 12932359]

Arguello A, Yang X, Vogt D, Stanco A, Rubenstein JL, Cheyette BN. Dapper antagonist of catenin-1 cooperates with Dishevelled-1 during postsynaptic development in mouse forebrain GABAergic interneurons. PLoS ONE. 2013; 8:e67679. [PubMed: 23826333]

Armstrong C, Szabadics J, Tamás G, Soltesz I. Neurogliaform cells in the molecular layer of the dentate gyrus as feed-forward γ-aminobutyric acidergic modulators of entorhinal-hippocampal interplay. J Comp Neurol. 2011; 519:1476–1491. [PubMed: 21452204]

Azim E, Jabaudon D, Fame RM, Macklis JD. SOX6 controls dorsal progenitor identity and interneuron diversity during neocortical development. Nat Neurosci. 2009; 12:1238–1247. [PubMed: 19657336]

Batista-Brito R, Rossignol E, Hjerling-Leffler J, Denaxa M, Wegner M, Lefebvre V, Pachnis V, Fishell G. The cell-intrinsic requirement of Sox6 for cortical interneuron development. Neuron. 2009; 63:466–481. [PubMed: 19709629]

Biressi S, Messina G, Collombat P, Tagliafico E, Monteverde S, Benedetti L, Cusella De Angelis MG, Mansouri A, Ferrari S, Tajbakhsh S, et al. The homeobox gene Arx is a novel positive regulator of embryonic myogenesis. Cell Death Differ. 2008; 15:94–104. [PubMed: 17932502]

Cai Y, Zhang Q, Wang C, Zhang Y, Ma T, Zhou X, Tian M, Rubenstein JL, Yang Z. Nuclear receptor COUP-TFII-expressing neocortical interneurons are derived from the medial and lateral/caudal ganglionic eminence and define specific subsets of mature interneurons. J Comp Neurol. 2013; 521:479–497. [PubMed: 22791192]

Chao HT, Chen H, Samaco RC, Xue M, Chahrour M, Yoo J, Neul JL, Gong S, Lu HC, Heintz N, et al. Dysfunction in GABA signalling mediates autism-like stereotypies and Rett syndrome phenotypes. Nature. 2010; 468:263–269. [PubMed: 21068835]

Chen YJ, Vogt D, Wang Y, Visel A, Silberberg SN, Nicholas CR, Danjo T, Pollack JL, Pennacchio LA, Anderson S, et al. Use of "MGE enhancers" for labeling and selection of embryonic stem cell-

derived medial ganglionic eminence (MGE) progenitors and neurons. PLoS ONE. 2013; 8:e61956. [PubMed: 23658702]

Choi GB, Dong HW, Murphy AJ, Valenzuela DM, Yancopoulos GD, Swanson LW, Anderson DJ. Lhx6 delineates a pathway mediating innate reproductive behaviors from the amygdala to the hypothalamus. Neuron. 2005; 46:647–660. [PubMed: 15944132]

Chu Z, Galarreta M, Hestrin S. Synaptic interactions of late-spiking neocortical neurons in layer 1. J Neurosci. 2003; 23:96–102. [PubMed: 12514205]

Close J, Xu H, De Marco García N, Batista-Brito R, Rossignol E, Rudy B, Fishell G. Satb1 is an activity-modulated transcription factor required for the terminal differentiation and connectivity of medial ganglionic eminence-derived cortical interneurons. J Neurosci. 2012; 32:17690–17705. [PubMed: 23223290]

Cobos I, Calcagnotto ME, Vilaythong AJ, Thwin MT, Noebels JL, Baraban SC, Rubenstein JLR. Mice lacking Dlx1 show subtype-specific loss of interneurons, reduced inhibition and epilepsy. Nat Neurosci. 2005; 8:1059–1068. [PubMed: 16007083]

Cobos I, Borello U, Rubenstein JLR. Dlx transcription factors promote migration through repression of axon and dendrite growth. Neuron. 2007; 54:873–888. [PubMed: 17582329]

Colasante G, Collombat P, Raimondi V, Bonanomi D, Ferrai C, Maira M, Yoshikawa K, Mansouri A, Valtorta F, Rubenstein JLR, Broccoli V. Arx is a direct target of Dlx2 and thereby contributes to the tangential migration of GABAergic interneurons. J Neurosci. 2008; 28:10674–10686. [PubMed: 18923043]

Denaxa M, Kalaitzidou M, Garefalaki A, Achimastou A, Lasrado R, Maes T, Pachnis V. Maturation-promoting activity of SATB1 in MGE-derived cortical interneurons. Cell Rep. 2012; 2:1351–1362. [PubMed: 23142661]

Du T, Xu Q, Ocbina PJ, Anderson SA. NKX2.1 specifies cortical interneuron fate by activating Lhx6. Development. 2008; 135:1559–1567. [PubMed: 18339674]

Elshatory Y, Gan L. The LIM-homeobox gene Islet-1 is required for the development of restricted forebrain cholinergic neurons. J Neurosci. 2008; 28:3291–3297. [PubMed: 18367596]

Flandin P, Kimura S, Rubenstein JL. The progenitor zone of the ventral medial ganglionic eminence requires Nkx2-1 to generate most of the globus pallidus but few neocortical interneurons. J Neurosci. 2010; 30:2812–2823. [PubMed: 20181579]

Flandin P, Zhao Y, Vogt D, Jeong J, Long J, Potter G, Westphal H, Rubenstein JLR. Lhx6 and Lhx8 coordinately induce neuronal expression of Shh that controls the generation of interneuron progenitors. Neuron. 2011; 70:939–950. [PubMed: 21658586]

Fragkouli A, van Wijk NV, Lopes R, Kessaris N, Pachnis V. LIM homeodomain transcription factor-dependent specification of bipotential MGE progenitors into cholinergic and GABAergic striatal interneurons. Development. 2009; 136:3841–3851. [PubMed: 19855026]

Gelman D, Griveau A, Dehorter N, Teissier A, Varela C, Pla R, Pierani A, Marín O. A wide diversity of cortical GABAergic interneurons derives from the embryonic preoptic area. J Neurosci. 2011; 31:16570–16580. [PubMed: 22090484]

Ghanem N, Jarinova O, Amores A, Long Q, Hatch G, Park BK, Rubenstein JL, Ekker M. Regulatory roles of conserved intergenic domains in vertebrate Dlx bigene clusters. Genome Res. 2003; 13:533–543. [PubMed: 12670995]

Grigoriou M, Tucker AS, Sharpe PT, Pachnis V. Expression and regulation of Lhx6 and Lhx7, a novel subfamily of LIM homeodomain encoding genes, suggests a role in mammalian head development. Development. 1998; 125:2063–2074. [PubMed: 9570771]

Han S, Tai C, Westenbroek RE, Yu FH, Cheah CS, Potter GB, Rubenstein JL, Scheuer T, de la Iglesia HO, Catterall WA. Autistic-like behaviour in Scn1a+/− mice and rescue by enhanced GABA-mediated neurotransmission. Nature. 2012; 489:385–390. [PubMed: 22914087]

Huang ZJ, Di Cristo G, Ango F. Development of GABA innervation in the cerebral and cerebellar cortices. Nat Rev Neurosci. 2007; 8:673–686. [PubMed: 17704810]

Hunt RF, Girskis KM, Rubenstein JL, Alvarez-Buylla A, Baraban SC. GABA progenitors grafted into the adult epileptic brain control seizures and abnormal behavior. Nat Neurosci. 2013; 16:692–697. [PubMed: 23644485]

Jeong J, Li X, McEvilly RJ, Rosenfeld MG, Lufkin T, Rubenstein JL. Dlx genes pattern mammalian jaw primordium by regulating both lower jaw-specific and upper jaw-specific genetic programs. Development. 2008; 135:2905–2916. [PubMed: 18697905]

Kanatani S, Yozu M, Tabata H, Nakajima K. COUP-TFII is preferentially expressed in the caudal ganglionic eminence and is involved in the caudal migratory stream. J Neurosci. 2008; 28:13582–13591. [PubMed: 19074032]

Kimura N, Ueno M, Nakashima K, Taga T. A brain region-specific gene product Lhx6.1 interacts with Ldb1 through tandem LIM-domains. J Biochem. 1999; 126:180–187. [PubMed: 10393337]

Lee S, Hjerling-Leffler J, Zagha E, Fishell G, Rudy B. The largest group of superficial neocortical GABAergic interneurons expresses ionotropic serotonin receptors. J Neurosci. 2010; 30:16796–16808. [PubMed: 21159951]

Liodis P, Denaxa M, Grigoriou M, Akufo-Addo C, Yanagawa Y, Pachnis V. Lhx6 activity is required for the normal migration and specification of cortical interneuron subtypes. J Neurosci. 2007; 27:3078–3089. [PubMed: 17376969]

Long JE, Cobos I, Potter GB, Rubenstein JLR. Dlx1&2 and Mash1 transcription factors control MGE and CGE patterning and differentiation through parallel and overlapping pathways. Cereb Cortex. 2009; 19(Suppl 1):i96–i106. [PubMed: 19386638]

Ma T, Zhang Q, Cai Y, You Y, Rubenstein JLR, Yang Z. A subpopulation of dorsal lateral/caudal ganglionic eminence-derived neocortical interneurons expresses the transcription factor Sp8. Cereb Cortex. 2012; 22:2120–2130. [PubMed: 22021915]

Madisen L, Zwingman TA, Sunkin SM, Oh SW, Zariwala HA, Gu H, Ng LL, Palmiter RD, Hawrylycz MJ, Jones AR, et al. A robust and high-throughput Cre reporting and characterization system for the whole mouse brain. Nat Neurosci. 2010; 13:133–140. [PubMed: 20023653]

Maroof AM, Keros S, Tyson JA, Ying SW, Ganat YM, Merkle FT, Liu B, Goulburn A, Stanley EG, Elefanty AG, et al. Directed differentiation and functional maturation of cortical interneurons from human embryonic stem cells. Cell Stem Cell. 2013; 12:559–572. [PubMed: 23642365]

McKinsey GL, Lindtner S, Trzcinski B, Visel A, Pennacchio LA, Huylebroeck D, Higashi Y, Rubenstein JL. Dlx1&2-dependent expression of Zfhx1b (Sip1, Zeb2) regulates the fate switch between cortical and striatal interneurons. Neuron. 2013; 77:83–98. [PubMed: 23312518]

Miyoshi G, Fishell G. GABAergic interneuron lineages selectively sort into specific cortical layers during early postnatal development. Cereb Cortex. 2011; 21:845–852. [PubMed: 20732898]

Miyoshi G, Hjerling-Leffler J, Karayannis T, Sousa VH, Butt SJB, Battiste J, Johnson JE, Machold RP, Fishell G. Genetic fate mapping reveals that the caudal ganglionic eminence produces a large and diverse population of superficial cortical interneurons. J Neurosci. 2010; 30:1582–1594. [PubMed: 20130169]

Nicholas CR, Chen J, Tang Y, Southwell DG, Chalmers N, Vogt D, Arnold CM, Chen YJ, Stanley EG, Elefanty AG, et al. Functional maturation of hPSC-derived forebrain interneurons requires an extended timeline and mimics human neural development. Cell Stem Cell. 2013; 12:573–586. [PubMed: 23642366]

Potter GB, Petryniak MA, Shevchenko E, McKinsey GL, Ekker M, Rubenstein JLR. Generation of Cre-transgenic mice using Dlx1/Dlx2 enhancers and their characterization in GABAergic interneurons. Mol Cell Neurosci. 2009; 40:167–186. [PubMed: 19026749]

Pueyo JI, Couso JP. Chip-mediated partnerships of the homeodomain proteins Bar and Aristaless with the LIM-HOM proteins Apterous and Lim1 regulate distal leg development. Development. 2004; 131:3107–3120. [PubMed: 15175252]

Rubenstein JL, Merzenich MM. Model of autism: increased ratio of excitation/inhibition in key neural systems. Genes Brain Behav. 2003; 2:255–267. [PubMed: 14606691]

Rudy B, Fishell G, Lee S, Hjerling-Leffler J. Three groups of interneurons account for nearly 100% of neocortical GABAergic neurons. Dev Neurobiol. 2011; 71:45–61. [PubMed: 21154909]

Sánchez-Alcañiz JA, Haege S, Mueller W, Pla R, Mackay F, Schulz S, López-Bendito G, Stumm R, Marín O. Cxcr7 controls neuronal migration by regulating chemokine responsiveness. Neuron. 2011; 69:77–90. [PubMed: 21220100]

Schönemeier B, Kolodzie A, Schul S, Jacob S, Hoell V, Stum R. Regional and cellular localization of the CXCl12/SDF-1 chemokine receptor CXCR7 in the developing and adult rat brain. J Comp Neurol. 2008; 510:207–220. [PubMed: 18615560]

Sierro F, Biben C, Martínez-Muñoz L, Mellado M, Ransohoff RM, Li M, Woehl B, Leung H, Groom J, Batten M, et al. Disrupted cardiac development but normal hematopoiesis in mice deficient in the second CXCL12/SDF-1 receptor, CXCR7. Proc Natl Acad Sci USA. 2007; 104:14759–14764. [PubMed: 17804806]

Stumm RK, Zhou C, Ara T, Lazarini F, Dubois-Dalcq M, Nagasawa T, Höllt V, Schulz S. CXCR4 regulates interneuron migration in the developing neocortex. J Neurosci. 2003; 23:5123–5130. [PubMed: 12832536]

Sussel L, Marin O, Kimura S, Rubenstein JL. Loss of Nkx2.1 homeobox gene function results in a ventral to dorsal molecular respecification within the basal telencephalon: evidence for a transformation of the pallidum into the striatum. Development. 1999; 126:3359–3370. [PubMed: 10393115]

Tiveron MC, Rossel M, Moepps B, Zhang YL, Seidenfaden R, Favor J, König N, Cremer H. Molecular interaction between projection neuron precursors and invading interneurons via stromal-derived factor 1 (CXCL12)/CXCR4 signaling in the cortical subventricular zone/ intermediate zone. J Neurosci. 2006; 26:13273–13278. [PubMed: 17182777]

Tricoire L, Pelkey KA, Daw MI, Sousa VH, Miyoshi G, Jeffries B, Cauli B, Fishell G, McBain CJ. Common origins of hippocampal Ivy and nitric oxide synthase expressing neurogliaform cells. J Neurosci. 2010; 30:2165–2176. [PubMed: 20147544]

Tricoire L, Pelkey KA, Erkkila BE, Jeffries BW, Yuan X, McBain CJ. A blueprint for the spatiotemporal origins of mouse hippocampal interneuron diversity. J Neurosci. 2011; 31:10948–10970. [PubMed: 21795545]

Vintersten K, Monetti C, Gertsenstein M, Zhang P, Laszlo L, Biechele S, Nagy A. Mouse in red: red fluorescent protein expression inmouse ES cells, embryos, and adult animals. Genesis. 2004; 40:241–246. [PubMed: 15593332]

Vokes SA, Ji H, McCuine S, Tenzen T, Giles S, Zhong S, Longabaugh WJR, Davidson EH, Wong WH, McMahon AP. Genomic characterization of Gli-activator targets in sonic hedgehog-mediated neural patterning. Development. 2007; 134:1977–1989. [PubMed: 17442700]

Wang Y, Li G, Stanco A, Long JE, Crawford D, Potter GB, Pleasure SJ, Behrens T, Rubenstein JLR. CXCR4 and CXCR7 have distinct functions in regulating interneuron migration. Neuron. 2011; 69:61–76. [PubMed: 21220099]

Wonders CP, Anderson SA. The origin and specification of cortical interneurons. Nat Rev Neurosci. 2006; 7:687–696. [PubMed: 16883309]

Xu Q, Tam M, Anderson SA. Fate mapping Nkx2.1-lineage cells in the mouse telencephalon. J Comp Neurol. 2008; 506:16–29. [PubMed: 17990269]

Yizhar O, Fenno LE, Prigge M, Schneider F, Davidson TJ, O'Shea DJ, Sohal VS, Goshen I, Finkelstein J, Paz JT, et al. Neocortical excitation/inhibition balance in information processing and social dysfunction. Nature. 2011; 477:171–178. [PubMed: 21796121]

Zerucha T, Stuhmer T, Hatch G, Park BK, Long Q, Yu G, Gambarotta A, Schultz JR, Rubenstein JL, Ekker M. A highly conserved enhancer in the Dlx5/Dlx6 intergenic region is the site of cross-regulatory interactions between Dlx genes in the embryonic forebrain. J Neurosci. 2000; 20:709–721. [PubMed: 10632600]

Zhao Y, Marín O, Hermesz E, Powell A, Flames N, Palkovits M, Rubenstein JL, Westphal H. The LIM-homeobox gene Lhx8 is required for the development of many cholinergic neurons in the mouse forebrain. Proc Natl Acad Sci USA. 2003; 100:9005–9010. [PubMed: 12855770]

Zhao Y, Flandin P, Long JE, Cuesta MD, Westphal H, Rubenstein JLR. Distinct molecular pathways for development of telencephalic interneuron subtypes revealed through analysis of Lhx6 mutants. J Comp Neurol. 2008; 510:79–99. [PubMed: 18613121]

Zhou FM, Hablitz JJ. Rapid kinetics and inward rectification of miniature EPSCs in layer I neurons of rat neocortex. J Neurophysiol. 1997; 77:2416–2426. [PubMed: 9163367]
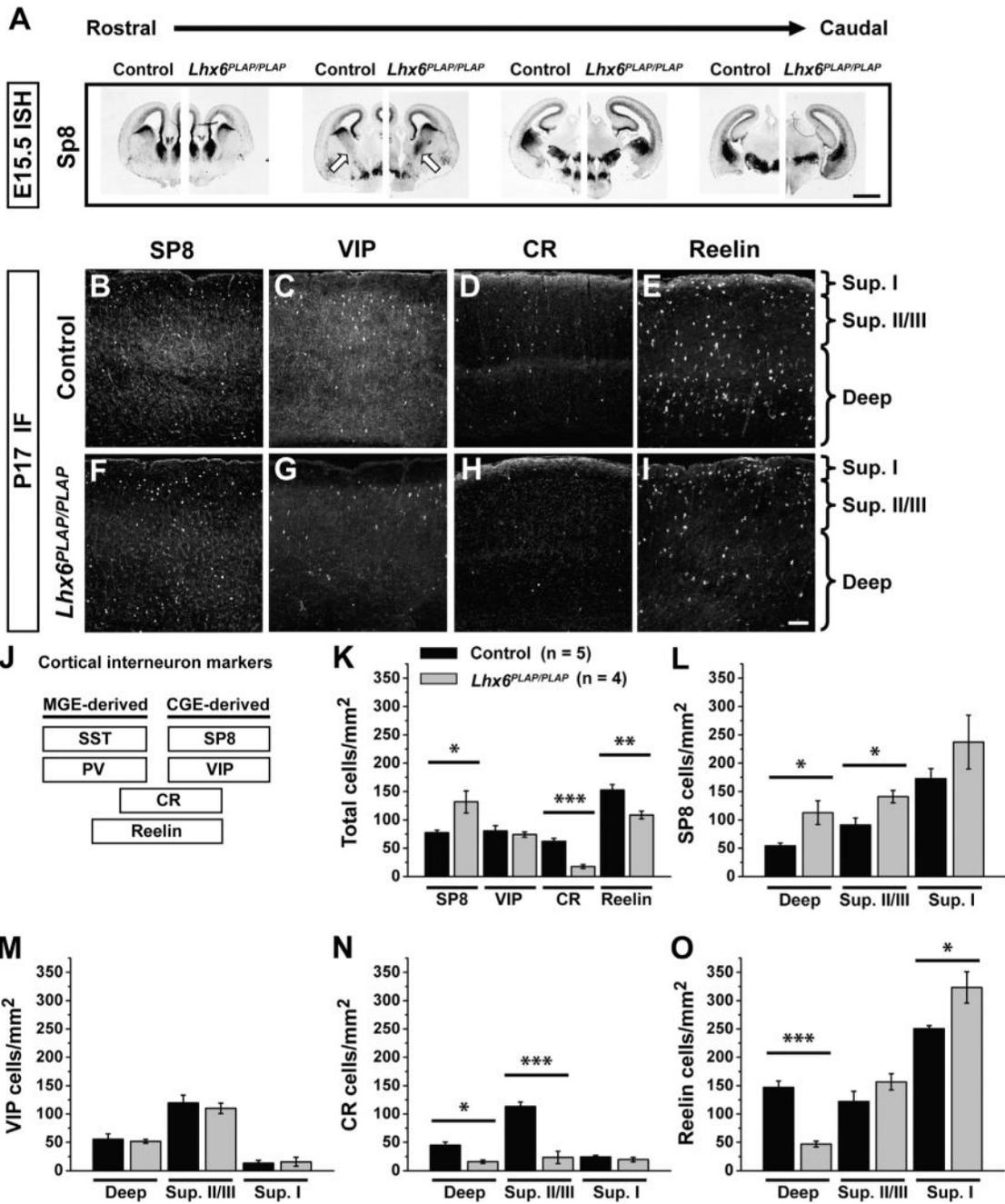
Figure 1. *Lhx6^PLAP/PLAP* **Progenitors and Interneurons Show a Partial Respecification of MGE-to-CGE Fate**

(A) Rostral to caudal series showing in situ hybridization (ISH) for SP8 in control (left) and *Lhx6^PLAP/PLAP* (right) E15.5 coronal hemisections. Arrows point to the MGE; the mutant has ectopic Sp8 expression. Scale bar represents 1 mm.

(B–I) Immunofluorescent (IF) images of CGE markers in the neocortex of control (B–E) and *Lhx6* mutant (F–I) coronal sections at P17. Scale bar in (I) represents 100 μm.

(J) Legend depicting relative distribution of molecular markers for MGE- and CGE-derived interneurons.

(K–O) Cell density quantification for VIP, CR, reelin, and Sp8. Cell density data shown for all layers (total) (K), superficial layers (sup. I and sup. II/III), and deep layers (deep) (L–O). Data are represented as mean ± SEM. One-way ANOVA was used to test significance among the groups: *p < 0.05, **p < 0.01, ***p < 0.001.
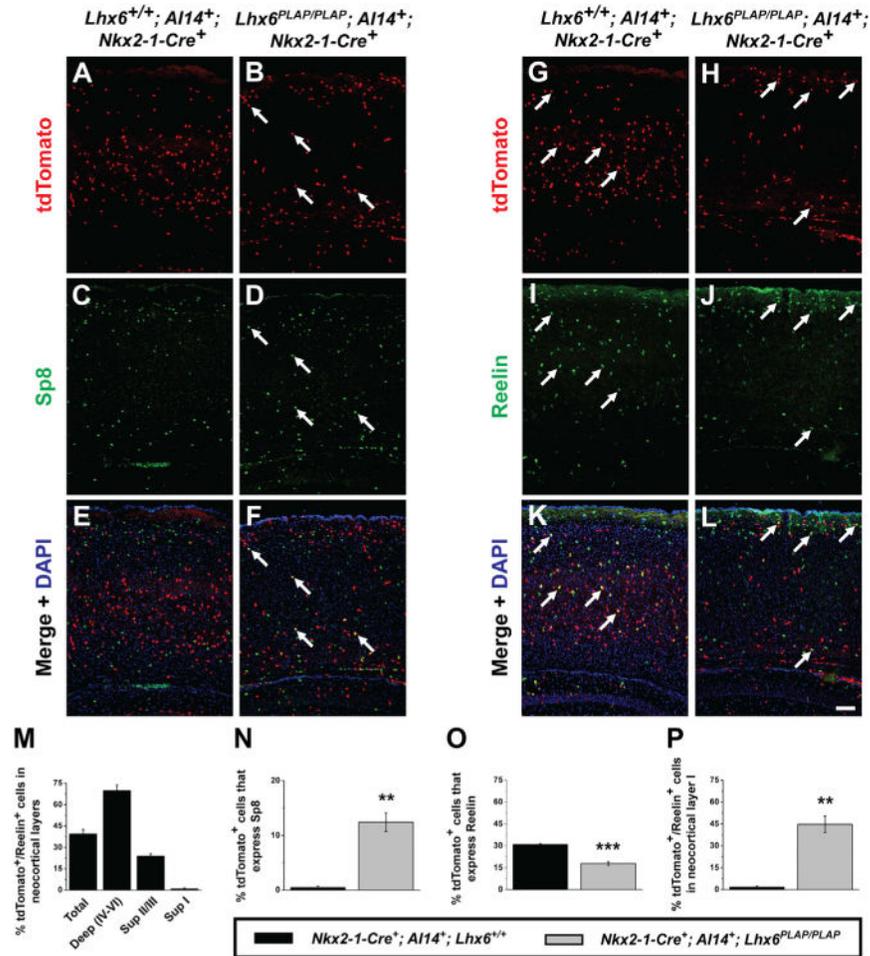See also Figure S1.

Figure 2. Fate Mapping of *Lhx6^{PLAP/PLAP}* MGE-Derived Cells Reveals a Subset that Expresses CGE Markers

(A–L) Immunofluorescent images of P13 WT or *Lhx6^{PLAP/PLAP}* neocortices from mice expressing *Nkx2-1-Cre* and the Cre-dependent tdTomato reporter (*Ai14*). MGE lineage cells (tdTomato$^+$) (A, B, G, and H) costained for Sp8 (C and D) or reelin (I and J). (E, F, K, and L) Merged images with DAPI (arrows point to examples of double-labeled cells). Scale bar in (L) represents 100 μm.

(M–P) Quantification of tdTomato$^+$/reelin$^+$ cells from WTs in neocortical layers. Quantification of the proportion of tdTomato$^+$ cells expressing Sp8 (N), reelin (O), and the proportion of tdTomato$^+$/reelin$^+$ cells in layer I (P). Data are represented as mean ± SEM. Student's t test was used to test significance among the groups: **p < 0.01, ***p < 0.001. See also Figure S2.
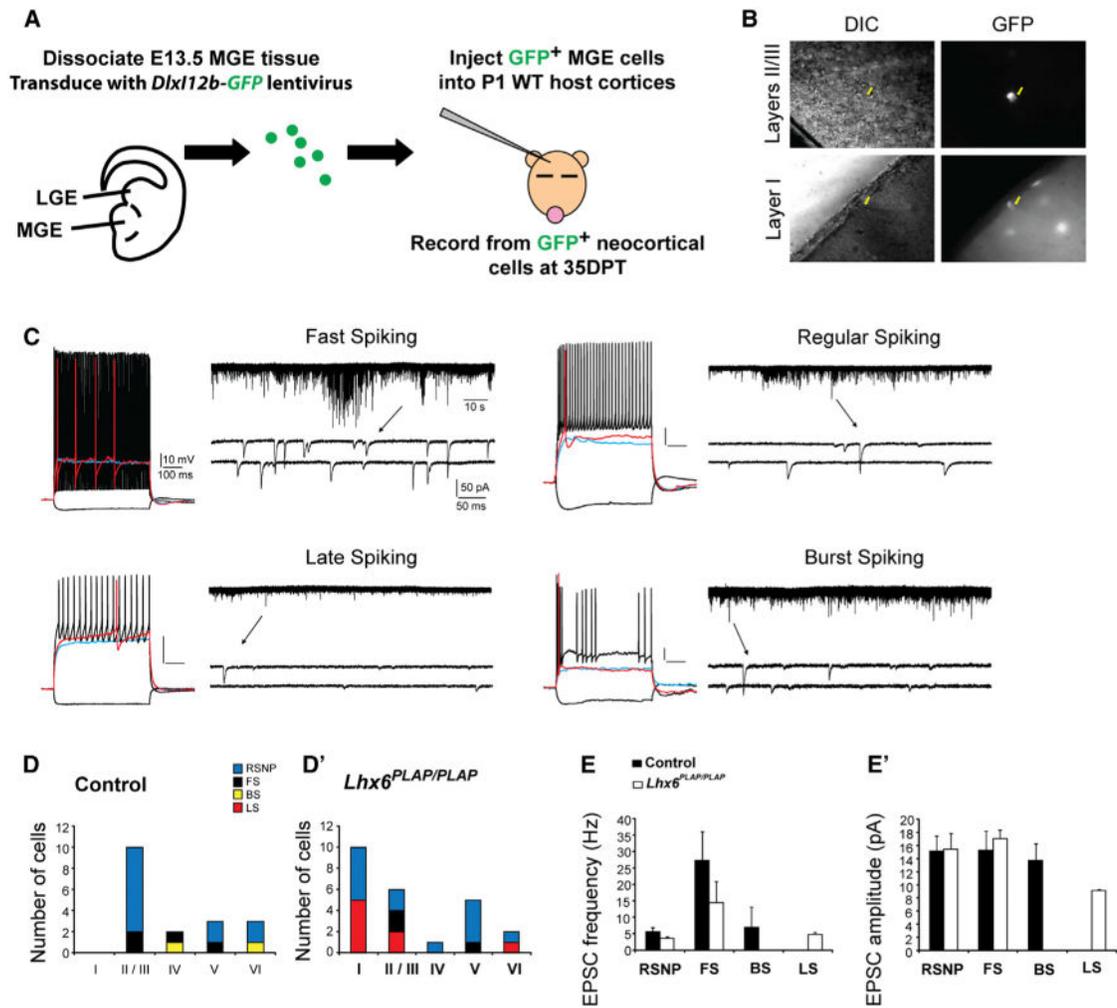
Figure 3. A Subset of *Lhx6$^{PLAP/PLAP}$* MGE-Derived Interneurons Exhibit Late-Spiking Properties

(A) Schema: lentiviral transduction of E13.5 WT and *Lhx6* mutant MGE cells by a GABAergic-specific GFP reporter; cells are then transplanted into P1 WT neocortex to develop. GFP$^+$ cells are assessed at 35 DPT.

(B) Images of GFP$^+$ cells recorded from neocortical layers II/III and I (yellow arrows indicate recording pipette tip).

(C) Electrophysiological responses of four different transplanted MGE-GABAergic neurons: fast spiking (FS), regular spiking (RS), late spiking (LS), and burst spiking (BS). Current-clamp traces (left side) following a hyperpolarizing current pulse (−50 pA; black) and depolarizing pulses at subthreshold (blue), near threshold (red), and near maximal firing (black). Shown on right: 2 min voltage-clamp recordings of sEPSCs for each cell. A region of each trace is expanded below (arrows) to show event waveforms.

(D and D′) Histograms summarizing the subgroups of recorded neurons in each layer.

(E and E′) Mean sEPSC frequency and amplitude for each interneuron subgroup. Data are represented as mean ± SEM.
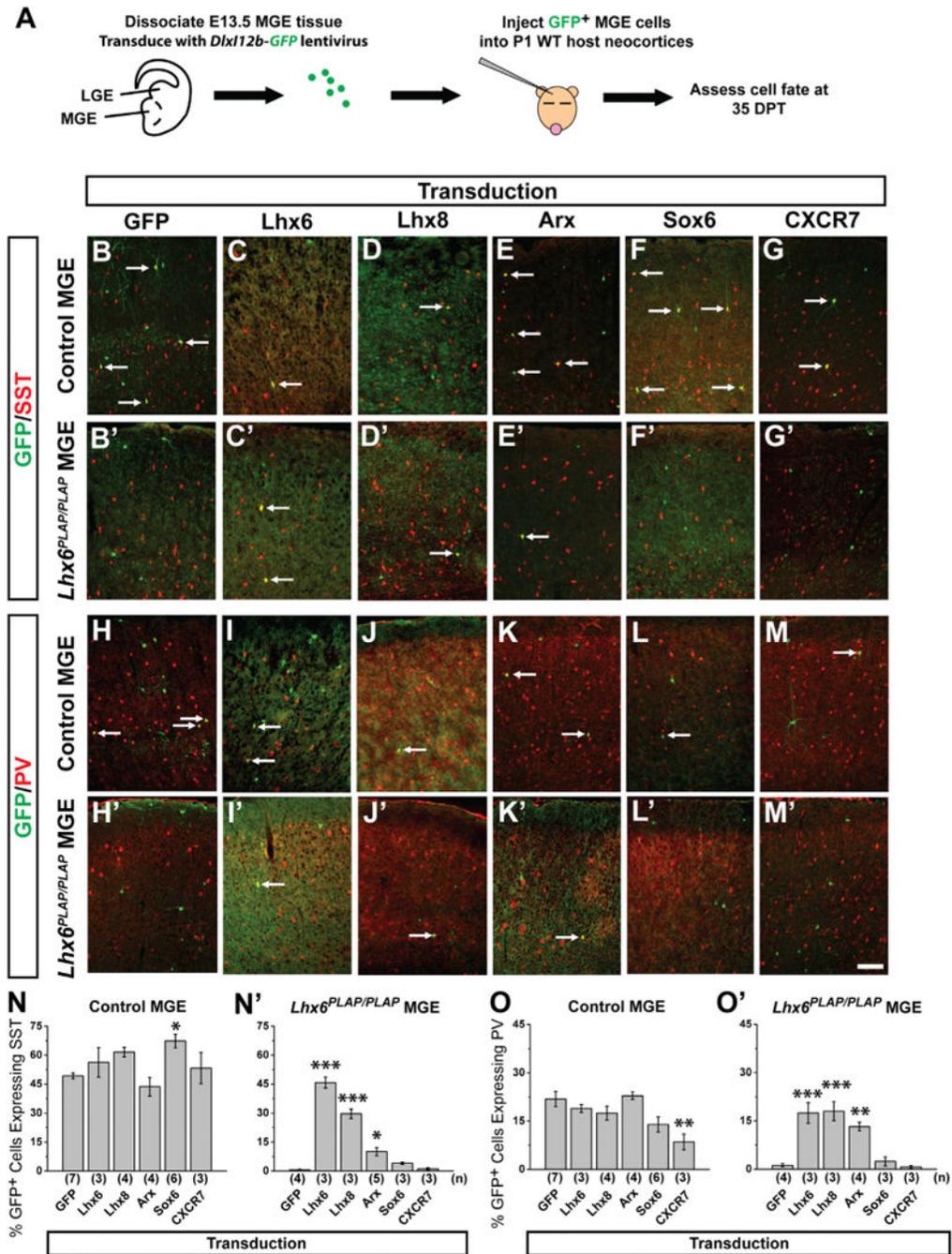
See also Figure S3 and Table S1.

Figure 4. Rescue of *Lhx6*^{PLAP/PLAP} Cell Fate Phenotypes via Transduction of Lhx6, Lhx8, and Arx

(A) Schema: E13.5 WT and mutant MGE cells are transduced with viruses expressing coding regions for *GFP*, *Lhx6*, *Lhx8*, *Arx*, *Sox6*, or *CXCR7*, and transplanted into P1 WT hosts. GFP⁺ cells are assessed at 35 DPT for SST or PV expression.

(B–M′) Immunofluorescence showing merged staining of GFP (green) with SST or PV (red) in the neocortex of controls (B–M) and *Lhx6*$^{PLAP/PLAP}$ (B′–M′). Scale bar in (M′) represents 100 μm.

(N and N′) Proportion of GFP⁺ cells that express SST for control (N) and *Lhx6$^{PLAP/PLAP}$* (N′) transplants.

(O and O′) Proportion of GFP⁺ cells that express PV for control (O) and *Lhx6$^{PLAP/PLAP}$* (O′) transplants. Data are represented as mean ± SEM. One-way ANOVA was used to test significance among the groups: $*p < 0.05$, $**p < 0.01$, $***p < 0.001$ compared to GFP transduction alone. Arrows point to GFP⁺ cells that coexpress the indicated marker. See also Figures S3–S5.
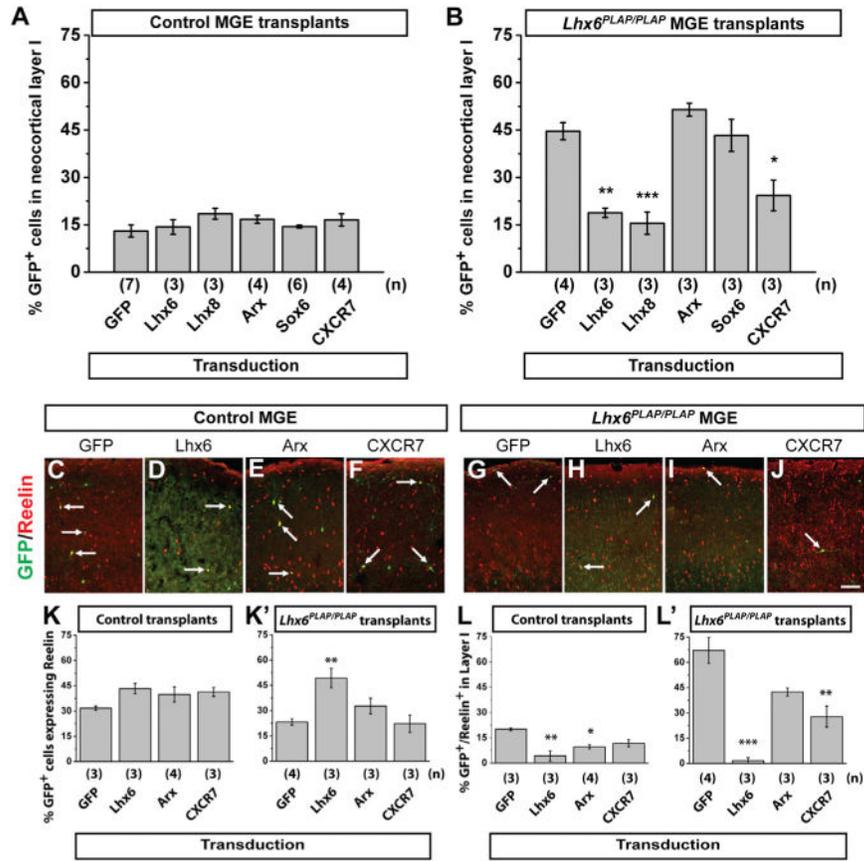
Figure 5. Rescue of *Lhx6^PLAP/PLAP^* Lamination Deficits via Transduction of Lhx6, Lhx8, and CXCR7

Proportion of transduced cells at 35 DPT that occupy neocortical layer I for control (A) and *Lhx6^PLAP/PLAP^* (B) MGE transplants. Two color immunofluorescence showing merged staining for GFP (green) and reelin (red) in the neocortex at 35 DPT of control (C–F) or *Lhx6^PLAP/PLAP^* (G–J) transplants. Arrows point to double-labeled cells. Quantification of GFP^+^/reelin^+^ transplanted control (K) and *Lhx6^PLAP/PLAP^* (K′) cells. Quantification of transplanted GFP^+^/reelin^+^ control (L) or *Lhx6^PLAP/PLAP^* (L′) cells in layer I. Data are represented as mean ± SEM. One-way ANOVA was used to test significance among the groups: *p < 0.05, **p < 0.01, ***p < 0.001 compared to GFP transduction alone. Scale bar in (J) represents 100 μm.
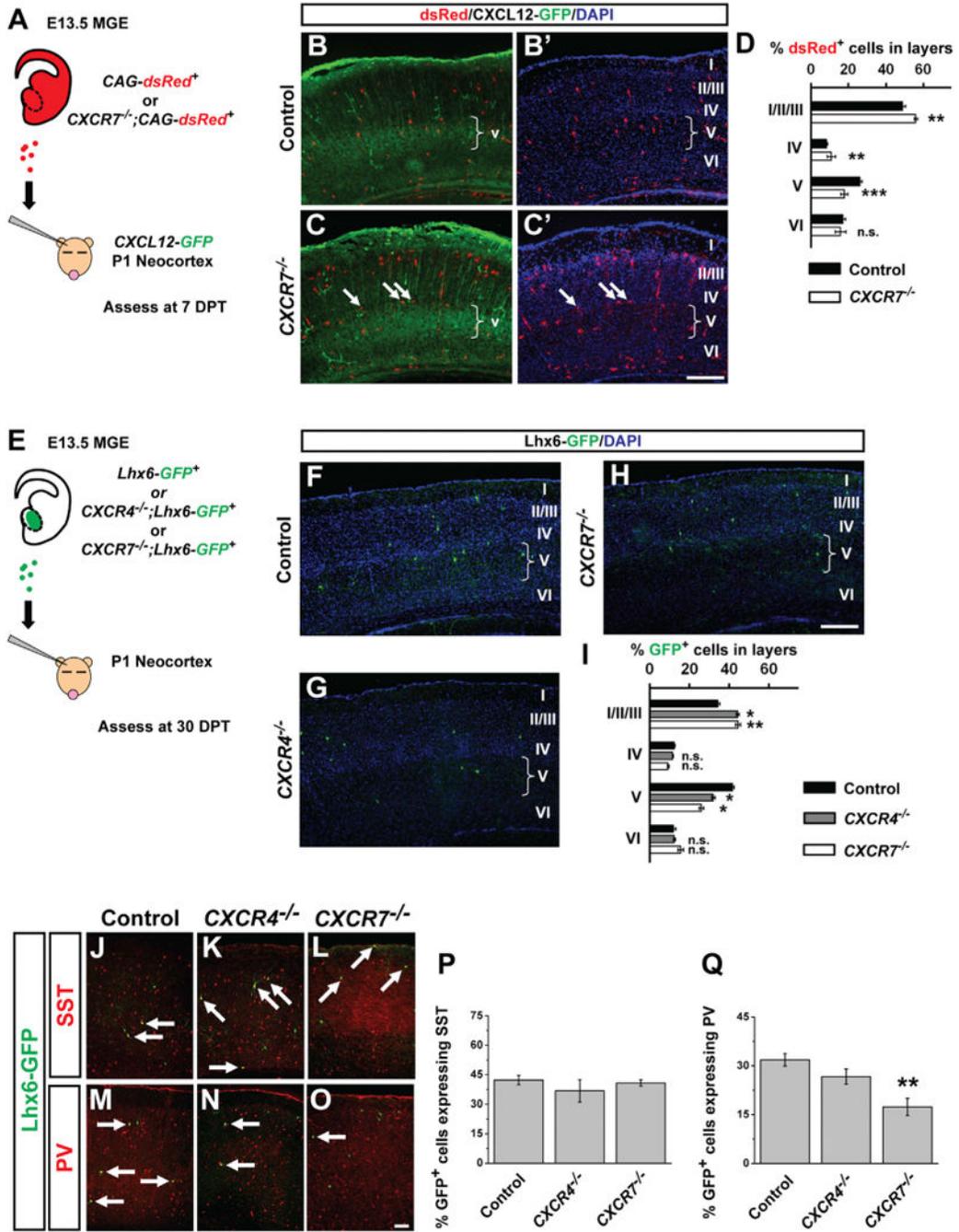
See also Figure S6.

Figure 6. *CXCR7* and *CXCR4* Regulate Laminar Position of Transplanted MGE Cells

(A) Schema depicting transplant of E13.5 *CAG-dsRed$^+$* MGE cells into P1 *CXCL12-GFP* reporter hosts.

(B–C′) Immunofluorescent images of transplanted MGE cells in the neocortex at 7 DPT, arrows in (C) and (C′) point to dsRed$^+$ cells at the IV/V border that lie outside of the CXCL12-GFP$^+$ domain in layer V. Brackets show the width of layer V. Scale bar in (C′) represents 250 μm.

(D) Quantification of *CAG-dsRed$^+$* cells in neocortical layers at 7 DPT.

(E) Schema depicting transplant of E13.5 *Lhx6-GFP*+ MGE cells into P1 WT hosts.

(F–H) Lhx6-GFP immunofluorescence (green) merged with DAPI (blue) in neocortex of mice in which either Control, *CXCR4*−/− or *CXCR7*−/− E13.5 *Lhx6-GFP*+ MGE cells were transplanted into P1 WT neocortex and assessed at 30 DPT. Scale bar in (H) represents 250 μm.

(I) Proportion of GFP+ Cells in Neocortical Layers of WT *CXCR4*−/− and *CXCR7*−/− MGE Cells

(J–Q) Immunofluorescence of 30 DPT transplants stained for SST (J–L) or PV (M–O), arrows point to coexpressing cells. Quantification of the proportion of Lhx6-GFP+ MGE cells that express SST (P) or PV (Q). Data are represented as mean ± SEM. Chi-square test (for lamination) or one-way ANOVA (for cell fate proportion) was used to test significance between groups. *$p < 0.05$, **$p < 0.01$, ***$p < 0.001$. Scale bar in (O) represents 100 μm. See also Figure S7.
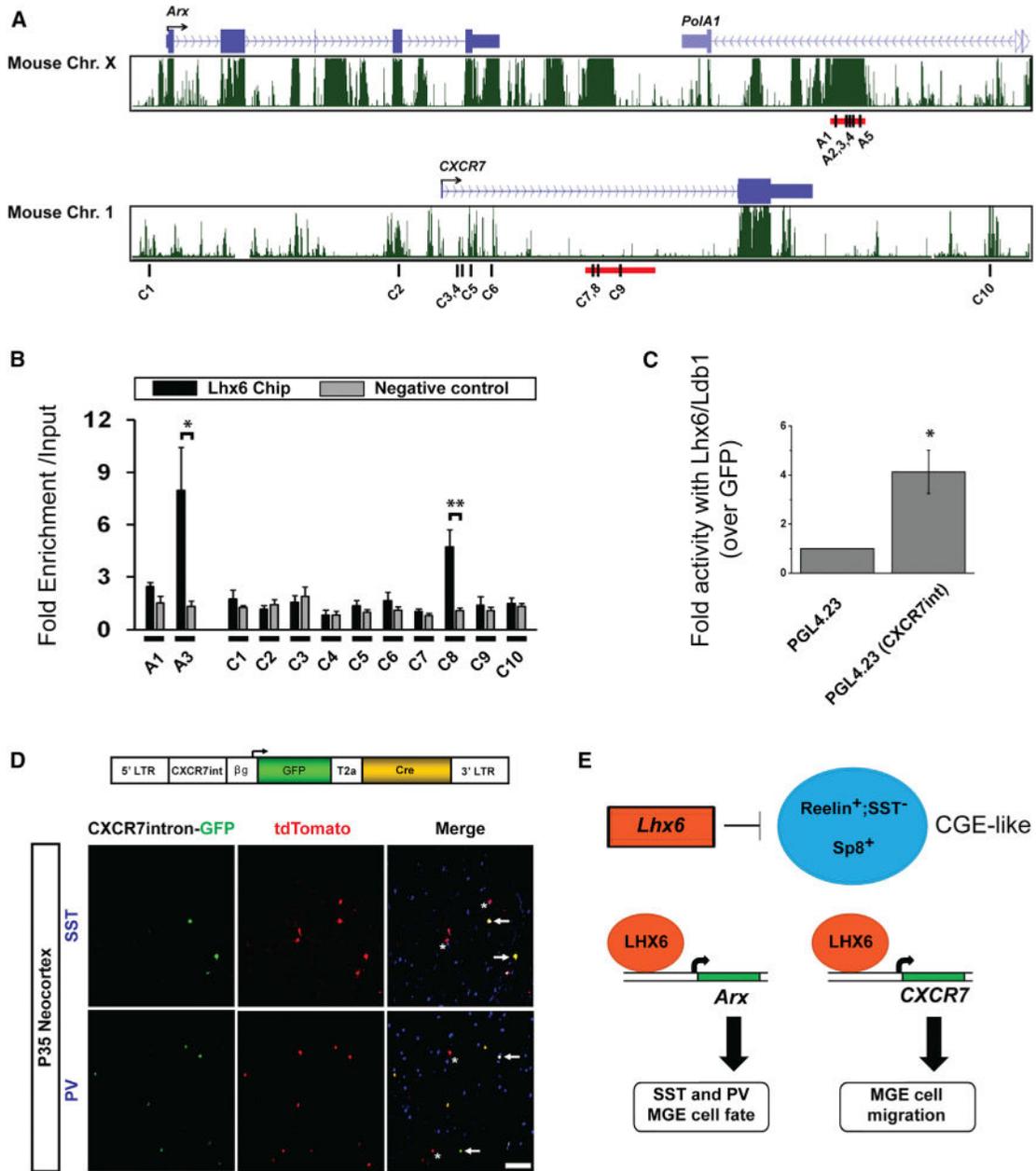
Figure 7. Lhx6 Directly Binds *Arx* and *CXCR7* Enhancers, and the *CXCR7* Enhancer Is Active in MGE Interneurons

(A) Genomic regions near *Arx* (top, MM9: 90,530,800–90,562,350) and *CXCR7* (bottom, MM9: 92,090,350–92,120,000) loci from University of California, Santa Cruz (UCSC) genome browser.

(B) LHX6 ChIP-qPCR assay for regions in the *Arx* enhancer (A1, 3), and the *CXCR7* locus (C1–10).

(C) Luciferase assay from P19 cells, transfected either with a *GFP* expression vector or *Lhx6-GFP* and *Ldb1* vectors in the presence of either a luciferase vector lacking an enhancer (PGL4.23) or a luciferase vector with the *CXCR7-intron* enhancer.

(D) *AI14*⁺ E13.5 MGE cells were transduced with a *CXCR7-intron-GFP-T2a-Cre* lentivirus (top) and transplanted into a WT P1 cortex. Immunofluorescence shows expression of 35 DPT coronal sections of GFP (green), tdTomato (red), and SST or PV (blue). Arrows point to cells expressing either SST or PV, and both GFP and tdTomato; asterisks mark cells only expressing tdTomato. Scale bar represents 100 μm.

(E) Model of *Lhx6* actions. *Lhx6* represses CGE-like interneuron fate. Lhx6 directly binds to enhancers near *Arx* and *CXCR7* to promote expression of these genes. ARX and CXCR7 are sufficient to rescue *Lhx6^{PLAP/PLAP}* MGE cell fate (SST and PV expression) and laminar distribution, respectively. Data are expressed as mean ± SEM. One-way ANOVA was used to test significance between groups. $*p < 0.05$, $**p < 0.01$.

See also Figure S8.